DOI: 10.1002/ejic.200801172

Laser CVD of Nanodisperse Ge–Sn Alloys Obtained by Dielectric Breakdown of SnH_4/GeH_4 Mixtures

Tomáš Křenek,[a,b] Petr Bezdička,[c] Nataliya Murafa,[c] Jan Šubrt,[c] and Josef Pola*[a]

Keywords: Germanium / Tin / Stannanes / Nanostructures / Alloys / Metastable compounds

TEA CO_2 laser-induced dielectric breakdown of an equimolar mixture of gaseous stannane and germane in Ar allows decomposition of both metal hydrides and chemical vapour deposition of the nanostructured Ge/Sn films. Analysis of the films by FTIR and Raman spectroscopy, X-ray diffraction analysis and electron microscopy revealed nanoregions of crystalline Sn and Sn-rich Ge/Sn alloys surrounded by an amorphous Ge/Sn phase. The crystalline Ge/Sn nanoalloys contain different amounts of Sn incorporated into the Ge lattice and undergo changes in composition at temperatures as low as 200 °C.

Introduction

Search for novel alloys, especially their metastable forms and multiphase micro- and nanostructures, their formation, growth and morphological changes represents an active scientific area of advanced materials[1] and is expected to lead to new discoveries in fundamental and highly applied topics.

The formation of *bulk* $Sn_x Ge_{1-x}$ alloys[2] with the solid solubility limit of Ge in Sn diamond-cubic structure >1% is difficult due to (i) large lattice mismatch (15%) between Ge and α-Sn and (ii) instability of d-c α-Sn phase at ambient temperature. There is, however, great interest in the Sn_xGe_{1-x} alloys with nonequilibrium composition of both elements (higher Ge content in the solid phase), because these alloys have a great potential (e.g., see ref.[3–5]) of a tunable direct energy gap. Such alloys can be fabricated only as metastable nanosized films by using special techniques allowing nonequilibrium growth.

Up to now, coevaporation of Sn and Ge and deposition to substrates kept at 100 K allowed[6] formation of amorphous single phase ($x \leq 0.15$) films, sputtering resulted in deposition of amorphous[7] and single-crystal or polycrystalline films ($x \leq 0.15$),[8] molecular beam epitaxy (MBE) enabled the growth of homogeneous crystalline ($x = 0.2–0.5$)[9–11] and fully strained ($x \leq 0.26$)[12] films on Ge, InSb[13] ($x \leq 0.1$) and CdTe[14] substrates, ion-assisted MBE yielded[15] crystalline d-c films ($x = 0.3–0.34$) on Ge, ultrahigh-vacuum chemical vapour deposition from Ge_2H_6 and SnD_4 precursors allowed synthesis of crystalline strain-free films ($x \leq 0.20$) on silicon substrates[16–18] and, finally, pulsed laser annealing of amorphous Ge/Sn films resulted in the formation of metastable crystalline features with $x = 0.22$ on glass[5] and even $x = 0.55$ on Ge[19] substrates.

Another laser technique enabling kinetic rather than thermodynamic control of the process is IR laser-induced gas-phase codecomposition of two different molecules,[20,21] which is capable of simultaneously generating clusters of several (two or more different) metals that will interact in the gas phase to yield "mixed nanosized systems" and deposit as such from the gas phase. This process experiences very high heating and cooling rates,[22,23] occurs within the order of microseconds and is feasible for the formation of metastable structures.

Here we report on a novel approach to chemical vapour deposition of Sn/Ge metastable alloys through gas-phase codecomposition of SnH_4 and GeH_4 by IR laser-induced dielectric breakdown and show that this technique is a suitable method to obtain nanostructured films composed of crystalline Sn and Ge/Sn alloy nanoobjects in the amorphous Ge/Sn phase.

Results and Discussion

The unfocused transversely excited atmospheric (TEA) CO_2 laser irradiation of SnH_4 and GeH_4 (both 5 Torr) in Ar (total pressure 110 Torr) does not lead to direct multiphoton excitation and decomposition of these compounds, as both molecules do not possess absorption bands in the laser emission region (Figure 1).

[a] Laboratory of Laser Chemistry, Institute of Chemical Process Fundamentals, Academy of Sciences of the Czech Republic, 16502 Prague, Czech Republic
E-mail:pola@icpf.cas.cz
[b] University of West Bohemia, 30614 Plzen, Czech Republic
[c] Institute of Inorganic Chemistry, Academy of Sciences of the Czech Republic, 25068 Řež, Czech Republic

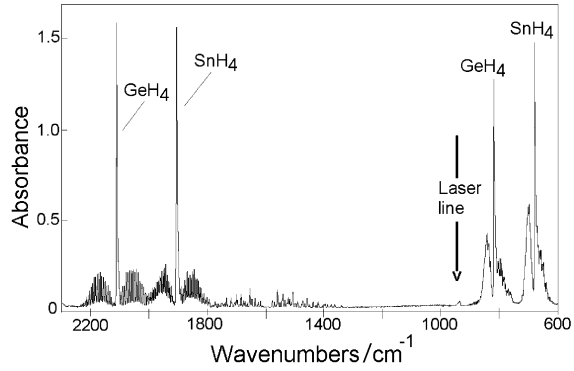

Figure 1. FTIR spectrum of SnH_4 and GeH_4 (both 5 Torr) in Ar (total pressure 110 Torr).

However, the highly focused radiation induces nonresonant interaction leading to dielectric breakdown[24,25] (a visible spark) and results in decomposition of both SnH_4 and GeH_4, yielding elemental metals in the gas phase and allowing deposition of ultrafine solid particles on the Si substrate. The absorption bands of the Ge and Sn precursors diminish at a similar rate and, respectively, deplete by 35 and 45% with 50 pulses, which indicates similar consumption of GeH_4 and SnH_4 for the formation of the solid deposit.

SEM images of the deposit (Figure 2) reveal fluffy morphology with submicrometre-sized bodies merging into several micrometre-large agglomerates. EDX-SEM analyses indicate small contamination by O and C elements and reveal stoichiometries ($Sn_{1.00}Ge_{0.95}Si_{10.60}C_{4,50}O_{1,94}$ for 300 μm^2 area and $Sn_{1.00}Ge_{0.88}Si_{0.15}$ $C_{0,51}O_{0,89}$ for several micrometre-sized particles) that agree with the relative decomposition of both metal hydrides as determined by FTIR spectra. The analyses also show that Sn/Ge particles do not cover the Si substrate completely.

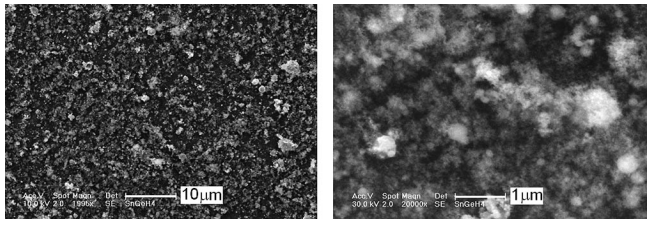

Figure 2. Typical SEM images of the deposit.

FTIR spectroscopy of the deposited film does not give any evidence on Sn–H and Ge–H bonds typical[26] for Sn_xGe_{1-x}:H films and confirms complete elimination of H from both precursors.

The Raman spectrum of the deposit (Figure 3) shows a broad band at 282–288 cm^{-1} and a sharp band at 518–520 cm^{-1} with a shoulder at 490 cm^{-1}, which are, respectively, assigned to the Ge–Ge bond in a Sn/Ge alloy,[11] the Si–Si bond in the silicon substrate and the Si–Si bond in Si/M (M = Sn,[27] Ge[28]) alloys. The Ge–Ge band being shifted from that of pure Ge (ca. 300 cm^{-1}) corresponds[11] to the Sn_xGe_{1-x} alloy with x = 0.17–0.25. The positions of the (Si–Si)* and (Ge–Ge)* bands (Figure 3) thus indirectly reveal the presence of Si/M (M = Sn, Ge) and Ge/Sn alloys, although Si–Ge, Si–Sn and Ge–Sn Raman modes are not observed.

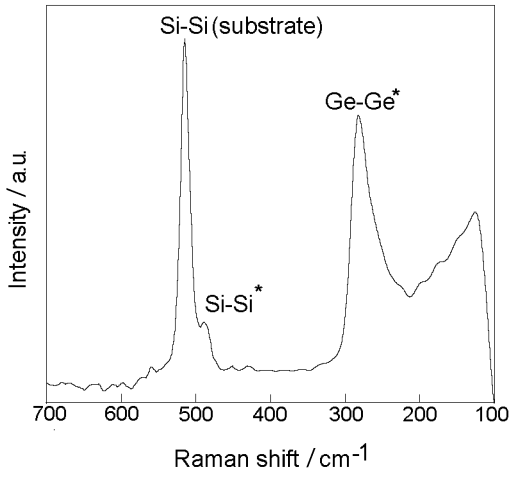

Figure 3. Typical Raman spectrum of the deposit. [The bands designated as (Si–Si)* and (Ge–Ge)*, respectively, occur in Si/M (M = Sn, Ge) and Ge/Sn alloys.].

Both vibrational spectra do not indicate the presence of interstitial hydrogen. [Although this species has not yet been detected for Sn and Ge/Sn, it is infrared active in Ge at 700 and 1880 cm^{-1} (ref.[29]) and Raman active at 745, 1794 and 3630 cm^{-1} (refs.[29,30])].

μ-XRD analysis (Figure 4a) reveals the presence of two crystalline phases, one with the unit cell parameters a = 0.5831 nm and c = 0.3182 nm, which corresponds to tetragonal β-Sn (designated as T and existing at temperatures >13.25 °C) and another corresponding to the Ge/Sn alloy (designated as G and G′). The bifurcated signal of the alloy can be deconvoluted to two peaks corresponding to the unit cell parameter a = 0.57552 and 0.59181 nm. These values are significantly higher than the unit cell parameter of pure diamond-type cubic Ge (a = 0.5657 nm) and they reflect, in agreement with the literature,[27] approximately 10% and far more (above 25%) incorporation of Sn atoms into the

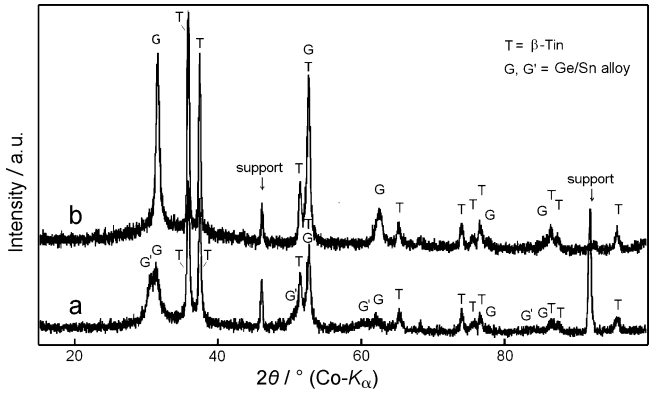

Figure 4. μ-XRD analysis of the deposit before (a) and after (b) heating to 200 °C.

Ge lattice. The bifurcated signal becomes single after heating to 200 °C (Figure 4b), in which case the peak corresponds to the unit cell parameter a = 0.57201 nm and approximately 7% incorporation of Sn atoms into the Ge lattice. We note that weight fractions of the crystalline Sn (ca. 30%) and Ge/Sn alloy (ca. 50%), as well as amorphous content (ca. 20%), estimated by Rietveld refinement procedure before and after heating are virtually the same. These results are supported by analysis by transmission electron microscopy.

The TEM image (Figure 5a) reveals irregular agglomerates consisting of uniform plate-like crystalline nanoparticles (10–50 nm). The marked places are point-out areas from which the EDS analyses, indicating great amounts of Ge and Sn elements and small contaminations of O and C, were carried out. The HRTEM images (Figure 5b–d) are consistent with a blend of crystalline and amorphous phase. Figure 5b shows the HRTEM micrograph of a crystalline nanoparticle with the interlayer spacing of d = 0.279 nm, the value corresponding to tetragonal Sn (PDF 04-0673). Figure 5c shows the HRTEM micrograph of a crystalline nanoparticle with the interlayer spacing of d = 0.339 nm, which corresponds to cubic Ge with d = 0.326 nm (PDF 04-0545). As agreed with μ-XRD analysis, the slight increase in the interlayer spacing can be explained by the Sn atoms incorporated into the Ge lattice. A very interesting HRTEM micrograph (Figure 5d) reveals the occurrence of a crystalline nanoparticle with two different values of interlayer spacing (d_1 = 0.330 nm and d_2 = 0.349 nm) and it is in line with different extents of Sn incorporation in the Ge lattice.

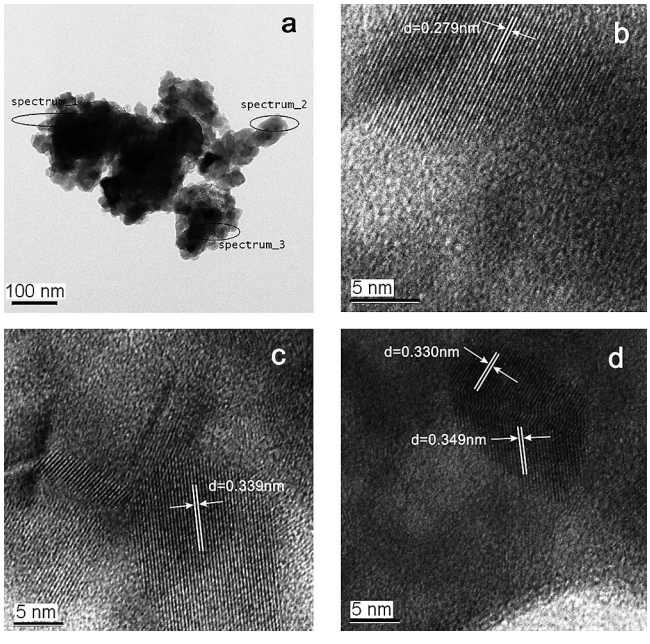

Figure 5. TEM (a) and HRTEM (b–d) micrographs of the deposit.

We assume that the presence of different Ge/Sn alloys is in keeping with a nonuniform temperature and possible transient (both neutral and charged) particles profiles in dielectric breakdown. The μ-XRD analysis of the deposit before and after heating to 200 °C is consistent with moderate temperature relaxation of nanoalloy structures and composition changes leading to separation of both alloy constituents, which occur rather as surface than bulk process.[31,32]

Conclusions

In conclusion, we have demonstrated that IR laser dielectric breakdown in an equimolar gaseous mixture of SnH_4/GeH_4 in Ar allows gas-phase deposition of nanoparticles containing crystalline Sn and metastable Sn-rich Ge/Sn alloys along with a Sn/Ge amorphous phase. These nanoparticles have to be formed upon decomposition of both metal hydrides and intermixing/clustering of extruded metal atoms in the gas phase. The Ge/Sn nanoalloys possess different contents of Sn incorporated in the Ge lattice and are modified in composition at temperatures as low as 200 °C.

Experimental Section

Laser irradiation of an equimolar mixture of SnH_4/GeH_4 (both 5 Torr) in Ar (total pressure 110 Torr) leading to dielectric breakdown in this mixture was accomplished with a TEA CO_2 laser (Plovdiv University, model 1300 M) operating with a repetition frequency of 1 Hz at the P(20) line of the $00^01 \rightarrow 10^00$ transition (944.19 cm^{-1}) and pulse energy 1.8 J. The gaseous mixture was irradiated in a Pyrex reactor (520 mL in volume, Figure 6) that consisted of two orthogonally positioned Pyrex tubes (both 3 cm in diameter, one 9 cm and the other 13 cm long) fitted with KBr windows and furnished with a PTFE valve connected to a vacuum manifold and pressure transducer. The laser pulse was focused with a NaCl lens (f.l. 15 cm) to generate a spark in the centre of the tube, above which was accommodated a silicon substrate. The mixture was irradiated with 45 pulses, and the thin film on the Si substrate was deposited through 3 cycles.

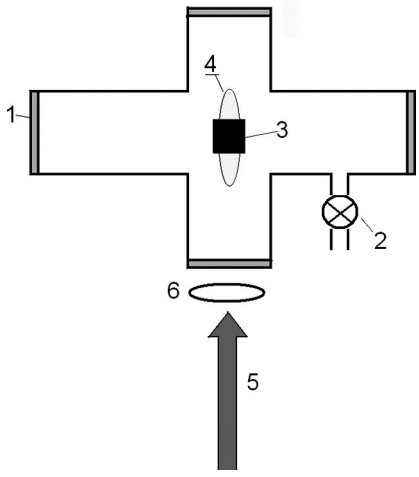

Figure 6. Top view of the irradiated Pyrex reactor: (1) KBr window; (2) PTFE valve; (3) substrate; (4) spark; (5) laser pulse; (6) lens.

The progress of codecomposition of SnH_4 and GeH_4 was monitored by FTIR spectroscopy (Nicolet Impact spectrometer) by using absorption bands at 677 cm^{-1} and 1902 cm^{-1} (SnH_4) and 816 cm^{-1} and 2108 cm^{-1} (GeH_4). Thereafter, the reactor was evacu-

ated and the Si substrate was transferred in sealed vials under Ar to prevent its oxidation for the measurements of its properties by different physical methods.

SEM analyses were carried out with a Philips XL30 CP scanning electron microscope and energy dispersive X-ray (EDX) analyses were conducted with a Philips XL30 CP instrument equipped with an EDX detector PV 9760 by using an accelerating voltage of 5–30 kV.

TEM (transmission electron microscopy) and HRTEM (high-resolution transmission electron microscopy) micrographs were carried out with a JEOL JEM 3010 microscope operated at 300 kV (LaB_6 cathode, point resolution 1.7 Å) with an EDX (energy dispersive X-ray) detector attached. A copper grid coated with a holey carbon film was used to prepare the samples. A fine powder of deposit was transferred onto a grid and used for the TEM observation.

Raman spectra were measured with a dispersive Raman instrument Nicolet Almega XR with the excitation wavelength 473 nm and power 10 mW. Spectra were collected in 32 expositions with a resolution of 2 cm^{-1}.

Diffraction patterns were collected with a PANalytical X′Pert PRO diffractometer equipped with a conventional X-ray tube (Co-K_α radiation, 40 kV, 30 mA, point focus), an X-ray monocapillary with a diameter of 0.1 mm and a multichannel detector X′Celerator with an antiscatter shield. A sample holder for single-crystal XRD measurement was adopted by adding z (vertical) axis adjustments (Huber 1005 goniometer head). The angle of the incident beam (ω) was fixed to 2° to suppress the penetration depth and enhance the signal of the assumed thin layer. XRD patterns were taken between 15 and 100° 2θ with 0.0167° step and 2100 s counting time per step that produces the total counting time of about 24 h. XRD patterns were not pretreated before interpretation, as no background correction was needed.

Qualitative analysis was performed with HighScore software package (PANalytical, The Netherlands, version 1.0d), Diffrac-Plus software package (Bruker AXS, Germany, version 8.0) and JCPDS PDF-2 database.[33] These analytical methods were also applied to the deposited films heated for 1 h at 200 °C in an evacuated ampoule.

For quantitative analysis of the XRD patterns, we used Diffrac-Plus Topas (Bruker AXS, Germany, version 4.1) with structural models based on the ICSD database.[34] This program permits the unit cell parameters to be determined, allows the weight fractions of crystalline phases to be estimated and also allows the amorphous content (the "degree of crystallinity" procedure) to be estimated by the Rietveld refinement procedure.

Stannane was prepared by treating tin tetrachloride with lithium aluminium hydride[35] and germane was obtained by reaction between germanium dioxide and potassium tetrahydroborate.[36] Both gases were distilled on vacuum line and checked for purity by FTIR spectroscopy.

Acknowledgments

This work was supported by Ministry of Education, Youth and Sports of the Czech Republic (Grant no. LC523).

[1] For example: J. K. Wessel (Ed.), *Handbook of Advanced Materials*, Wiley-Interscience, Hoboken, **2004**.

[2] *SGTE Alloy Phase Diagrams Databases*, **2004**.
[3] D. V. Jenkins, J. D. Dow, *Phys. Rev. B* **1987**, *36*, 7994–8000.
[4] G. He, H. A. Atwater, *Phys. Rev. Lett.* **1997**, *79*, 1937–1940.
[5] S. Oguz, W. Paul, T. F. Deutsch, B. Y. Tsaur, D. V. Murphy, *Appl. Phys. Lett.* **1984**, *43*, 848–850.
[6] J. C. Bennet, R. F. Egerton, *Vacuum* **1996**, *47*, 1419–1422.
[7] H. Fukumoto, H. Myoren, T. Nakashita, T. Imura, Y. Osaka, *Jpn. J. Appl. Phys.* **1986**, *25*, 1312–1346.
[8] S. I. Shah, J. E. Greene, L. L. Abels, Q. Yao, P. M. Raccah, *J. Cryst. Growth* **1987**, *83*, 3–10.
[9] H. Höchst, M. A. Engelhardt, I. Hérnandey-Calderón, *Phys. Rev. B* **1989**, *40*, 9703–9708.
[10] R. R. Pukite, A. Harwit, S. S. Iyer, *Appl. Phys. Lett.* **1989**, *54*, 2142–2144.
[11] M. Rojas-López, H. Navarro-Contreras, P. Desjardins, O. Gurdal, N. Taylor, J. R. A. Carlsson, J. E. Grene, *J. Appl. Phys.* **1998**, *84*, 2219–2223.
[12] O. Gurdal, P. Desjardins, J. R. A. Carsson, N. Taylor, H. H. Radamson, J.-E. Sundgren, J. E. Greene, *J. Appl. Phys.* **1998**, *83*, 162–170.
[13] M. T. Asom, E. A. Fitzgerald, A. R. Kortan, B. Spear, L. C. Kimerling, *Appl. Phys. Lett.* **1989**, *55*, 578–579.
[14] R. C. Bowman, P. M. Adams, M. A. Engelhardt, H. Höchst, *J. Vac. Sci. Technol. A* **1990**, *8*, 1577–1581.
[15] G. He, H. A. Atwater, *Appl. Phys. Lett.* **1996**, *68*, 664–666.
[16] M. R. Bauer, J. Tolle, A. V. G. Chizmeshya, S. Zollner, J. Menendez, J. Kouvetakis, *Mater. Res. Symp. Proc.* **2003**, *744*, 49–54.
[17] M. R. Bauer, J. Tolle, C. Bungay, A. V. G. Chizmeshya, D. J. Smith, J. Menendez, J. Kouvetakis, *Solid State Commun.* **2003**, *127*, 355–359.
[18] C. J. Cook, S. Zollner, M. R. Bauer, P. Aella, J. Kouvetakis, J. Menendez, *Thin Solid Films* **2004**, *455–456*, 217–221.
[19] I. T. H. Chang, B. Cantor, *Thin Solid Films* **1993**, *230*, 167–178.
[20] J. Pola, D. Pokorná, M. J. Diánez, M. J. Sazagués, Z. Bastl, V. Vorlíček, *Appl. Organomet. Chem.* **2005**, *19*, 854–858.
[21] D. Pokorná, J. Boháček, V. Vorlíček, J. Šubrt, Z. Bastl, E. A. Volnina, J. Pola, *J. Anal. Appl. Pyrol.* **2006**, *75*, 65–68.
[22] D. F. McMillen, K. E. Lewis, G. P. Smith, D. M. Golden, *J. Phys. Chem.* **1982**, *86*, 709–718.
[23] D. K. Russell, *Chem. Soc. Rev.* **1990**, *19*, 407–437.
[24] A. M. Ronn, *Chem. Phys. Lett.* **1976**, *42*, 202–204.
[25] A. H. Schwebel, A. M. Ronn, *Chem. Phys. Lett.* **1983**, *100*, 178–182.
[26] E. Chin-Prado, R. S. Katiyar, W. Muñoz, O. Resto, S. Z. Weisz, *Phys. Rev. B* **1994**, *50*, 11653–11660.
[27] M. Bauer, C. Ritter, D. A. Crozier, J. Ren, J. Menendez, G. Wolf, J. Kouvetakis, *Appl. Phys. Lett.* **2003**, *83*, 2163–2165.
[28] J. Olivares, P. Martin, A. Rodriguez, J. Sangrador, J. Jimenez, T. Rodríguez, *Thin Solid Films* **2000**, *358*, 56–61.
[29] M. Budde, B. B. Nielsen, C. P. Cheney, N. H. Tolk, L. C. Feldman, *Phys. Rev. Lett.* **2000**, *85*, 2965–2968.
[30] J. Weber, M. Hiller, E. V. Lavrov, *Phys. B: Condensed Matter.* **2007**, *401–402*, 91–96.
[31] K. A. Mäder, A. Baldereschi, H. von Känel, *Solid State Commun.* **1989**, *69*, 1123.
[32] A. Roland, J. Bernardini, G. Moya, C. Girardeaux, *Surf. Sci.* **2004**, *566–568*, 1163.
[33] *JCPDS PDF-2 Database*, release 54, International Centre for Diffraction Data, Newton Square, PA, USA, **2004**.
[34] *ICSD Database FIZ Karlsruhe*, release 2008/1, Germany, **2008**.
[35] G. H. Reifenberg, W. J. Considine, *Organometallics* **1993**, *12*, 3015.
[36] W. I. Jolly, J. E. Drake, *Inorg. Synthesis* **1963**, *7*, 34–44.

Received: December 2, 2008
Published Online: March 12, 2009

